genesis 50:404–414 (2012)

ARTICLE

pangolin Expression Influences the Development of a Morphological Novelty: Beetle Horns

Bethany R. Wasik* and Armin P. Moczek

Department of Biology, Indiana University, Bloomington, Indiana

Received 2 July 2011; Revised 28 September 2011; Accepted 6 October 2011

Summary: Morphological diversity arises during development through the actions and interactions of diverse developmental pathways. Among those, the Wnt pathway is known to contribute to diverse developmental processes such as segmentation and the morphogenesis of appendages. Here, we characterize a transcription factor in the Wnt pathway, *pangolin* (*pan*), to investigate the role of Wnt signaling in the development of evolutionarily novel body structures: the horns of beetles. Beetle horns are highly diverse in size, shape, and number and develop principally from two major body regions: the head and prothorax. We investigate horns in two species of the genus *Onthophagus* using comparative in situ hybridization, larval RNA interference, and allometric measurements to analyze whether horn formation is regulated by *pan* and by extension the Wnt pathway. Our results illustrate that *pan* expression affects beetle horn growth in a species-, sex-, and location-specific manner in two morphologically distinct, yet closely-related, *Onthophagus* species. genesis 50:404–414, 2012. **© 2011 Wiley Periodicals, Inc.**

Key words: *Onthophagus*; RNA interference; appendage growth

INTRODUCTION

The development and diversification of novel traits is of great interest in evolutionary developmental biology. On a proximate level, novel traits allow us to explore the degree to which their development relies on the actions of either novel or pre-existing genes, developmental pathways, and pathway interactions. On an ultimate level, the evolution of novel traits allows us to investigate the genetic, developmental, or ecological events that may have mediated the origin of new genes and pathways or alternatively their reuse in a novel developmental context. Here, we focus on the role of the Wnt pathway in the development and diversification of a novel trait in insects: the beetle horn. Below we first introduce our study organisms and traits, then outline our rationale for investigating Wnt signaling during horn formation, and finally address the specific objectives of our study.

Several thousands of beetle species, including species in the genus *Onthophagus* studied here, express horns or horn-like structures. Horns are produced chiefly on the dorsal head and/or the dorsal prothorax (pronotum), body regions that traditionally lack major outgrowths. Consequently, beetle horns cannot be homologized easily with more traditional insect structures and are thus considered an evolutionary novelty. Importantly, great diversity exists among and within species with respect to location, size, shape, and number of horns. For instance, in many species, horns are expressed in a sexually dimorphic manner and often greatly exaggerated in males yet reduced or absent in females. Instances of reversed sexual dimorphisms also exist but are overall very rare. In addition, horns are frequently expressed in a dimorphic manner within the male sex, such that large males express disproportionately large horns, whereas small males express greatly

Additional Supporting Information may be found in the online version of this article.

*Correspondence to: Bethany R. Wasik, Department of Ecology and Evolutionary Biology, Yale University, 165 Prospect Street, Osborn Memorial Labs, New Haven, CT 06520-8106.

E-mail: bethany.wasik@gmail.com

Contract grant sponsor: NIH Genetics Training Grant, Contract grant number: 2T32 GMOO7757-29; Contract grant sponsor: NSF-IGERT Grant, Contract grant number: DGE-0504627; Contract grant sponsor: NSF grants, Contract grant number: IOS 0445661, IOS 0718522

Published online 13 October 2011 in
Wiley Online Library (wileyonlinelibrary.com).
DOI: 10.1002/dvg.20814

reduced or no horns (Arrow, 1951). In all species studied to date, horns were found to function as weapons in competition with conspecifics over breeding opportunities, typically involving pushing and shoving contests (Snell-Rood and Moczek, in press). However, despite the many unique attributes of beetle horns, their development resembles, at least superficially, that of traditional insect appendages such as legs, wings, and mouthparts.

For example, beetle horns originate from epidermal outbuddings undergo a short period of explosive growth immediately before the larval-pupal molt (the prepupal growth phase), which is then followed by a final period of sculpting or resorption (the pupal remodeling phase). Adult horn size and shape, therefore, emerge as the sum of both prepupal growth and pupal remodeling, similar to the development of traditional appendages. Even though beetle horns cannot be homologized with more traditional insect structures or appendages, these similarities to traditional appendage development indicate the possibility that horn growth and patterning may be regulated by some of the same developmental gene networks and mechanisms, such as the Wnt pathway. In this study, we investigate the role of the Wnt pathway in the regulation of horn growth in two-horned beetle species that have diverged in important aspects of horns expression, including the nature and degree of sexual dimorphism.

The Wnt pathway influences a range of early developmental processes such as segmentation and segment polarity, as well as later developmental events that produce vital organs (e.g., the heart) and appendages (e.g., wings and limbs) (reviewed in Bejsovec, 2006). In addition, the Wnt pathway has been shown to regulate the development of recent evolutionary inventions, such as wing spots in *Drosophila guttifera* (Werner *et al.*, 2010), sex-specific gemmae in ponerine ants (Baratte *et al.*, 2006), and eyespots and rays in butterflies (e.g., Carroll *et al.*, 1994).

In insects, Wnt signaling has been studied in great detail during segmentation and in the context of appendage formation, in particular with respect to the establishment of the proximodistal (PD) axis. Specifically, the Wnt signal transduction pathway overlaps with other patterning networks including the TGFβ pathway. Coexpression of both pathway ligands, *wingless* (*wg*) and *decapentaplegic* (*dpp*), promote *Distal-less* (*Dll*) expression in insects and determine where appendages will develop (Angelini and Kaufman, 2005b and citations therein; Diaz-Benjumea *et al.*, 1994).

Phenotypic effects of Wnt pathway mutants are diverse, including transformation of wings or halteres to thorax tissue (notum), duplications of limb PD axes resulting in branched distal limbs, abnormal development of head structures, and abnormal segmentation (Baker, 1988; Bolognesi *et al.*, 2008; Grossmann *et al.*, 2009; Morata and Lawrence, 1977; Ober and Jockusch, 2006). Here, we focus on the Wnt-pathway member *pangolin* (*pan*), which encodes a lymphoid enhancing factor/T-cell-specific transcription factor homolog that binds to other Wnt pathway components, such as *armadillo* (*arm*), to transcribe *wg* target genes in the nucleus (Bejsovec, 2006; Brunner *et al.*, 1997; Logan and Nusse, 2004). *pan* has been identified as an informative pathway member to examine Wnt pathway activity in appendage development, in addition to being shown in several insect taxa to affect segmentation early and appendage growth and patterning later in development (e.g., Angelini and Kaufman, 2005a; Bolognesi *et al.*, 2008; Brunner *et al.*, 1997). Here, we take advantage of these insights and examine *pan* expression and function in the context of horned beetle development to evaluate the role of Wnt signaling in horn development in particular and horned beetle appendage formation in general.

Specifically, we explore whether *pan* functions during horn development in two *Onthophagus* species (*O. binodis* and *O. sagittarius*; Fig. 1) that have diverged with respect to size, shape, and location of horn expression as well as the nature of sexual dimorphism in horn expression. Adult *O. binodis* express sexually dimorphic thoracic (pronotal) horns that are exaggerated in males and reduced to a ridge in females. In contrast, adult *O. sagittarius* express a rare reversed sexual dimorphism: adult females possess a single, large pronotal horn and a single large medial head horn, whereas males develop only minor paired pronotal outgrowths and small, paired head horns at the front dorsal edge of the head (Fig. 1). Both species belong to distinct clades within the genus *Onthophagus* and have diverged from a common ancestor ~40 million years ago (Emlen *et al.*, 2005). Our main objective is to characterize *pan* expression and function to begin understanding the potential contributions of Wnt signaling to the development and diversification of sex- and species-specific patterns of horn formation in these species and relative to presumed ancestral functions in the formation of antennae, mouthparts, eyes, wings, and limbs. Our results show that late-stage Wnt signaling appears to be pivotal for horn growth and remodeling in a species-, sex- and location-specific manner, in addition to the proper development of elytra, legs, and eyes.

RESULTS

Onthophagus *pan* Cloning and Sequence Analysis

We isolated two alternatively-spliced *pan* isoforms (termed *panA* and *panB* in Supporting Information Figs. 1 and 2) in both *O. binodis* and *O. sagittarius*. *panA* fragments cloned comprised 308 bp in *O. binodis* and 180 bp in *O. sagittarius* (Supporting Information

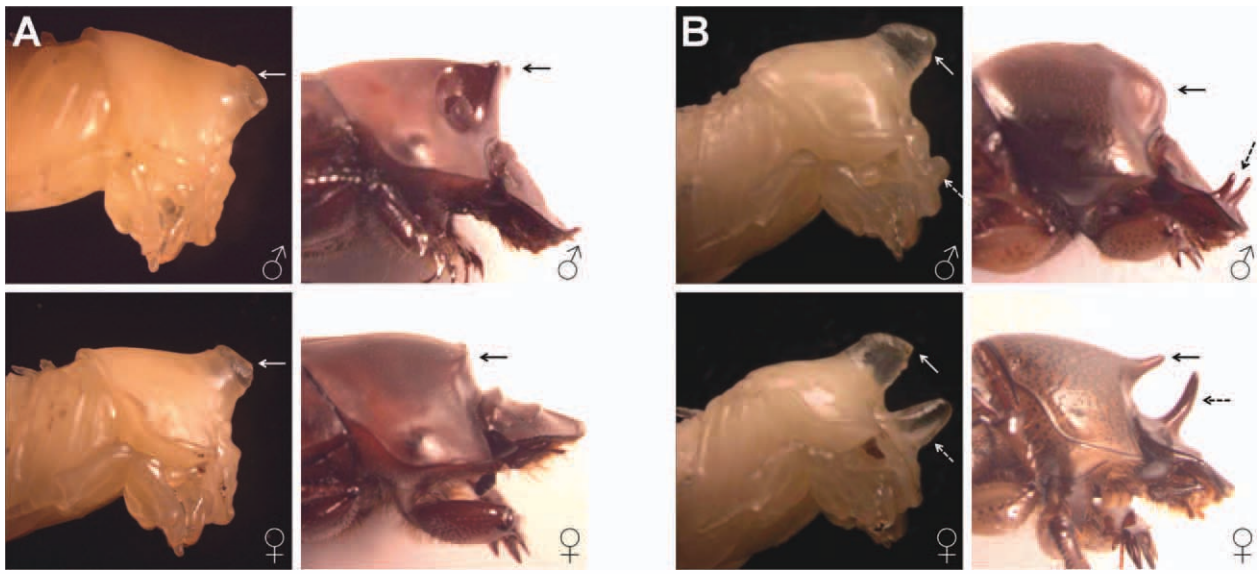

FIG. 1. Pupal and adult horn phenotypes in *O. binodis* and *O. sagittarius.* (**a**) *O. binodis* males and females exhibit similar pronotal horn growth during the prepupal stage, resulting in sexually monomorphic pupae (white arrows), but undergo sexually dimorphic horn resorption during pupal development, resulting in sexually dimorphic adults. In adults, males possess a broad pronotal horn, whereas females retain a pronotal ridge (black arrows). (**b**) In contrast, *O. sagittarius* exhibits a unique sex-reversed pronotal horn phenotype with females as the main horn-bearing sex. As with *O. binodis*, pronotal horn growth is similar in both sexes (white solid arrows) but is then followed by male-specific pronotal horn tissue resorption during the pupal stage. As a result, adult females possess a single, large pronotal horn, whereas males develop minor paired pronotal outgrowths, or ridges (black solid arrows). Additionally, both sexes develop sexually dimorphic head horns. Adult females develop a single large horn projection from the center of the dorsal head, and adult males develop small, paired head horns at the front dorsal edge of the head (black dashed arrows). In contrast to pronotal horns, minimal horn resorption occurs during head horn development, and adult head horn phenotypes are primarily the product of differential prepupal growth.

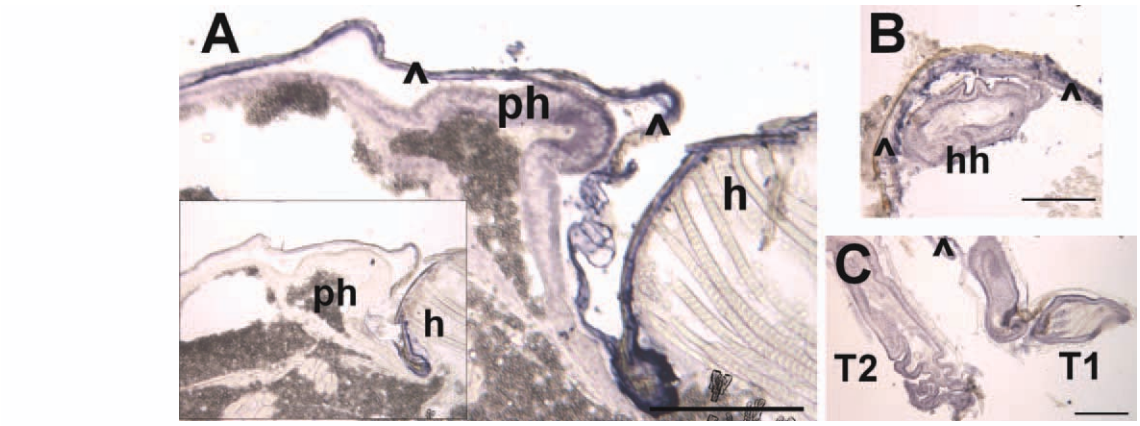

FIG. 2. *Onthophagus pan* mRNA expression. Shown are sagittal cryosections from prepupal *O. sagittarius* larvae stained with *Ospan* RNA probes (visualized in purple stain in tissue; boxed in black in Supporting Information Figures 1 and 2). In all images, the dorsal direction is up, anterior is right, and posterior is left, and in all images, carets denote nonspecific labeling in the overlaying cuticle. (**a**) *Ospan* mRNA expression was observed in the larval pronotal horn primordium (ph) (bottom left inset shows no signal in control horn section), (**b**) head horn primordium (hh), and (**c**) all leg sections (shown here are prothoracic (T1) and mesothoracic (T2) leg sections). Scale bars represent 200 μm.

Fig. 1A), whereas *panB* fragments comprised 296 bp in *O. binodis* and 179 bp in *O. sagittarius* (Supporting Information Fig. 2A). Although *pan* was characterized in both *Tribolium* and *Oncopeltus*, no published evidence exists suggesting alternative splicing in those insects (Angelini and Kaufman, 2005a; Bolognesi *et al.*, 2008). Therefore, we referenced isolated *Onthophagus pan* regions to *Drosophila* in which both *pan* isoforms are well documented, and the position of alternatively-splicing is known to be in exon 11 (Dooijes *et al.*, 1998;

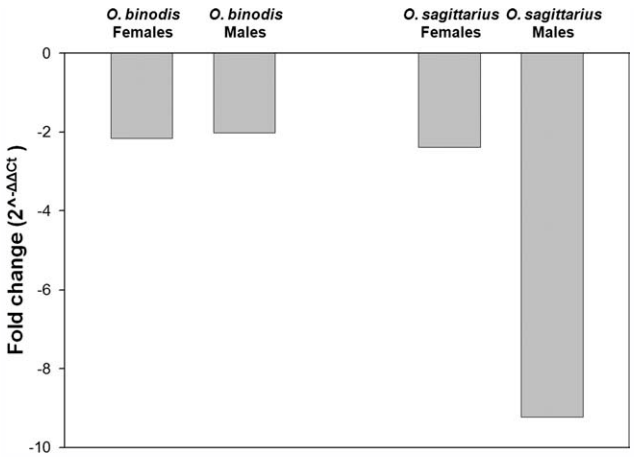

FIG. 3. Change of *pan* transcript abundance following RNAi. Shown are the fold changes, or reduction, in pan transcript abundance among *O. binodis* and *O. sagittarius* males and females following *pan* RNAi. All measures were determined using the $2^{\wedge -\Delta\Delta Ct}$ equation (see Methods), which incorporates both wild-type *pan* expression (from tissue in uninjected individuals) and β-*actin* expression (in all individuals). In all groups, *pan* is reduced following *pan* RNAi.

van de Wetering *et al.*, 1997). *O. binodis* and *O. sagittarius panA* fragments encode amino acids 279–380 and 279–338 in *Dm*pan, respectively (Isoform A; Genbank Accession Number: NP_726522). *O. binodis* and *O. sagittarius panB* fragments encode amino acids 279–376 and 279–333 in *Dm*pan, respectively (Isoform H; Genbank Accession Number: NP_001014685). *Ob*panA and *Os*panA proteins share 94% amino acid similarity with each other and 69.9% each to *Dm*panA. *Ob*panB and *Os*panB proteins share 94% amino acid similarity with each other and 69.9% each to *Dm*panH.

All *Onthophagus pan* sequences contained part of the high mobility group at the 5′ end (Hulo *et al.*, 2006), which functions as a DNA-binding domain (dashed box in Supporting Information Figs. 1B and 2B). Our *O. binodis pan* fragment contained a portion of the C-clamp, a cysteine-rich region that assists with DNA-binding at the 3′ end (underlined in Figures Supporting Information Figs. 2B and 3B; Chang *et al.*, 2008). Our sequences excluded the N-terminal region of the pan protein that binds to the β-catenin protein (armadillo in *Drosophila*) to actively transcribe *wg* target genes in the nucleus (Brunner *et al.*, 1997).

Onthophagus *pan* mRNA Expression

pan mRNA expression was observed in both species in regions of the larval epidermis undergoing growth, including head and thoracic structures (Fig. 2). Specifically, we observed *pan* mRNA in tissue of developing mouthparts and wings (not shown), pronotal horns, legs, and head horns in *O. sagittarius*. Examples of these observations are shown in Figure 2 for *O. sagittarius* larval sections. Negative controls with similar prepupal tissue sections displayed no expression (see inset in Fig. 2A).

pan RNAi

We did not observe any effect of ds*pan* injection location on the resulting RNAi phenotypes, similar to other *Onthophagus* RNAi studies (Moczek and Rose, 2009; Wasik and Moczek, 2011; Wasik *et al.*, 2010). Survival and penetrance values of control- and *pan* RNAi-injected animals are summarized in Supporting Information Table 2.

In both species, the strongest effects of *pan* RNAi were observed in elytra (forewings), and mild effects were observed in fore-tibia, tarsi, and eye development, all of which parallel phenotypes described in previous insect studies (Angelini and Kaufman, 2005a; Brunner *et al.*, 1997). Therefore, elytra were used as a primary phenotypic marker to determine whether adults were affected by *pan* RNAi, and measurements from pupae that developed into unaffected adults were not incorporated into our analyses, in addition to measurements from unaffected adults. Thus, we focused our analyses on data from (a) affected adults, (b) pupae that developed into affected adults, and (c) pupae that died before *pan* phenotypic characterization. For both species, we first detail our results from quantitative RT-PCR of *pan* transcript levels, followed by our results for morphological traits (wings, fore-tibia, and eyes) whose development in other species is known to be regulated by the Wnt pathway. We then present results for both pronotal and head horns, putative novel targets of *pan* signaling.

Quantitative RT-PCR Analyses

We developed primers targeting invariant sequence regions in both isoforms (Supporting Information Table 1; target sequence boundaries are denoted by asterisks (*) in Supporting Information Fig. 2C for *O. binodis* and Supporting Information Fig. 2D for *O. sagittarius*). Quantitative RT-PCR results showed a relative decrease in *pan* expression in thoracic tissue from *pan* RNAi individuals compared to β-*actin* in the same tissue sample, relative to *pan* and β-*actin* levels in wild-type thoracic tissue samples (see Fig. 3). Specifically following RNAi, *pan* transcript levels in male and female *O. binodis* exhibited a twofold reduction compared to *pan* levels in wild type. *Ospan* transcript depletion was more effective and resulted in a 9.23-fold and 2.39-fold reductions in male and female *pan* transcript levels, respectively. We compared *pan* expression levels between wild type and *pan* RNAi individuals using two-tailed *t*-tests. Our results showed normalized *pan* expression levels ($C_{t\ pan}/C_{t\ actin}$) in RNAi individuals of both species were significantly different ($P < 0.05$) compared to wild type (data not shown). Combined, these results

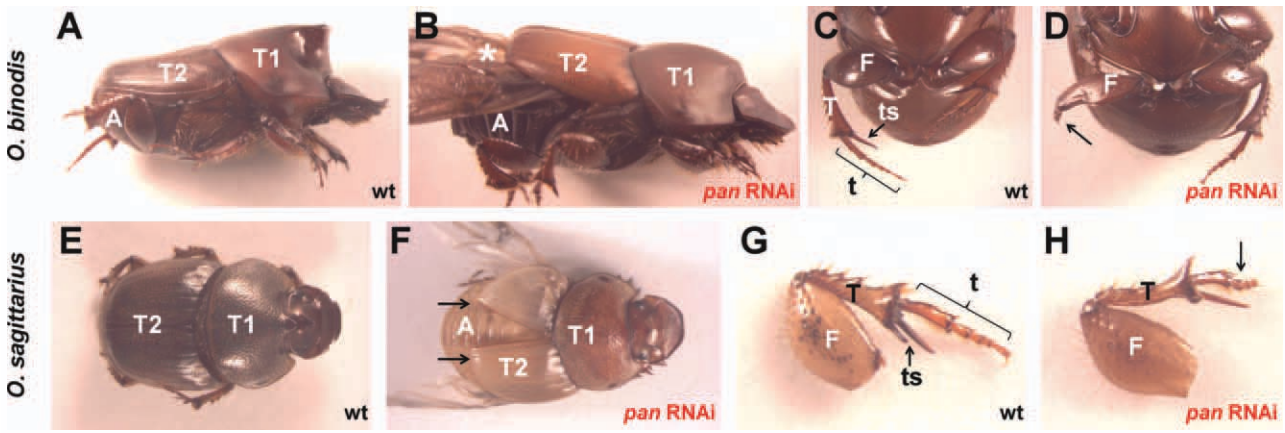

FIG. 4. *O. binodis* and *O. sagittarius* nonhorn *pan* RNAi phenotypes. (**a**) Lateral view of wild-type *O. binodis* male with prothorax (T1), mesothorax with elytra/forewings (T2), and abdomen (a) labeled. (**b**) *O. binodis* male after *pan* RNAi with visibly shortened elytra. Asterisk (*) denotes dorsal abdomen that is covered with elytra in wild type. (**c**) Ventral view of *O. binodis* wild-type metathoracic legs. Femur (F), tibia (T), tarsi (t), and tibial spurs (ts) are denoted. (**d**) *O. binodis pan* RNAi leg phenotype (black arrow) missing tibia and tarsi. (**e**) Dorsal view of an *O. sagittarius* wild-type female. (**f**) *O. sagittarius* female after *pan* RNAi with reduced elytra (similar to B). (**g**) Wild-type *O. sagittarius* mesothoracic leg. (**h**) *O. sagittarius* mesothoracic leg with *pan* RNAi phenotype. Reduced tarsi are denoted with black arrow. Anterior is right and posterior is left in all images, where applicable.

indicate that we were able to reduce *pan* transcript abundance with RNAi, albeit to different levels in different species.

Wing-, fore-tibia-, and eye-defects in *O. binodis*

We injected 229 *O. binodis* larvae with a ds*pan* construct that preceded variable regions among isoforms (boxed in Supporting Information Figs. 1 and 2). We observed no obvious morphological effects in pupae, whereas visible morphological effects were observed in 69 of the surviving 116 adults (59.5%) (Supporting Information Table 2). The most distinct adult morphological phenotypes were reduced, shortened elytra and in rare cases, abnormal distal leg segments (Fig. 4A–D). Prothoracic fore-tibia length was significantly reduced following *pan* RNAi in adult males ($P < 0.0001$) but not females (Supporting Information Fig. 3, Supporting Information Table 3). Furthermore, dorsal eye width was significantly reduced in both males ($P = 0.0010$) and females ($P = 0.0291$; Supporting Information Fig. 4, Supporting Information Table 4).

Wing-, fore-tibia- and eye-defects in *O. sagittarius*

We injected 125 *O. sagittarius* larvae with ds*pan* which resulted in 68 adults with observable morphological effects (54.4%) (Supporting Information Table 2). Similar to *O. binodis*, no major morphological effects were observed in pupal nonhorn structures. Adult phenotypes were similar to those described in *O. binodis* and consisted primarily of reduced elytra with additional minor abnormalities in mesothoracic tibiae and tarsi (Fig. 4E–H). In contrast to *O. binodis*, fore-tibia length of *O. sagittarius* was not significantly different in either males or females following *pan* RNAi (Supporting Information Fig. 3, Supporting Information Table 3). Also, we observed no significant effects on dorsal eye width in *pan* RNAi males or females (Supporting Information Fig. 4, Supporting Information Table 4).

pan RNAi Effects on Prepupal Pronotal Horn Growth

We used morphometric measurements and ANOVAs to compare pupal pronotal horn lengths from ds*pan*-injected and control-injected animals to quantify the extent of *pan* RNAi effects on prepupal pronotal horn growth (Fig. 5, Supporting Information Tables 5 and 6). In *O. binodis*, pupal pronotal horn length was significantly reduced in both males and females after *pan* RNAi compared to control-injected individuals ($P < 0.0001$; Fig. 5C). In contrast, pupal pronotal horn length in both *O. sagittarius* males and females was unaffected (Fig. 5C, Supporting Information Table 6), suggesting *pan* may affect prepupal pronotal horn growth differently in *O. binodis* and *O. sagittarius*.

pan RNAi Effects on Adult Pronotal Horn Development

In *O. binodis*, adult pronotal horn length in both males ($P < 0.0001$) and females ($P = 0.0003$) was significantly reduced (Fig. 5F, Supporting Information Table 5). Similarly, *O. sagittarius* also showed reduced pronotal horn length in both males ($P < 0.0005$) and females following *pan* RNAi ($p < 0.0001$; Fig. 5F, Supporting Information Table 6). Thus, *pan* RNAi affected prepupal pronotal horn growth only in *O. binodis* but adult pronotal horn development in both species.

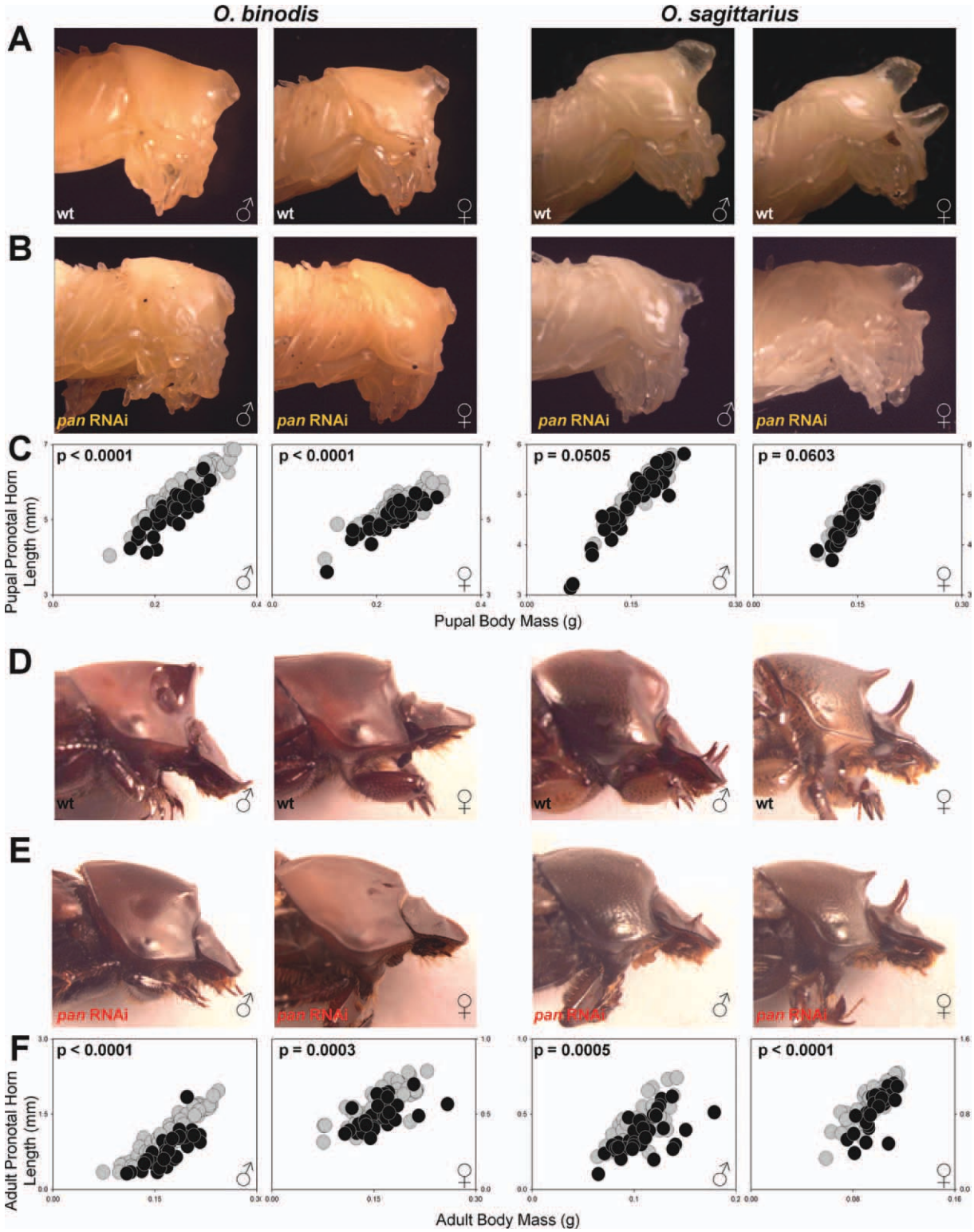

FIG. 5. *O. binodis* and *O. sagittarius* pronotal horn phenotypes and allometries. Left to right columns display *O. binodis* males, *O. binodis* females, *O. sagittarius* males, *O. sagittarius* females. In all images, anterior is right and posterior is left. (**a**) Wild-type pupal pronotal horn phenotypes. (**b**) Representative pronotal horn phenotypes in ds*pan*-injected pupae. (**c**) Allometric measurements for both pupal pronotal horn length with pupal body mass (g) on the *x* axis and pupal pronotal horn length (mm) on the *y* axis. Gray circles represent control-injected individuals, and black circles represent ds*pan*-injected individuals. (**d**) Wild-type adult pronotal horn phenotypes. (**e**) Representative *pan* RNAi adult pronotal horn phenotypes. (**f**) Allometric measurements for both adult pronotal horn length with adult body mass (g) on the *x* axis and adult pronotal horn length (mm) on the *y* axis.

pan RNAi Effects on Pupal Pronotal Horn Remodeling

To further dissect whether reduced adult horn length in *pan* RNAi animals may also be due to elevated pupal horn resorption, we calculated absolute and relative horn tissue loss that occurred during the pupal stage for both species. Both absolute and relative horn loss were significantly reduced, rather than elevated, in male and female *O. binodis* ($P < 0.0001$; Supporting Information Table 7). Similarly, female (but not male) *O. sagittarius* exhibited significantly reduced relative (but not absolute) horn loss ($P = 0.0139$) following *pan* RNAi (Supporting Information Table 8). Therefore, in females of both species and in *O. binodis* males, *pan* RNAi reduced pupal horn resorption well below what is normally observed in wild-type animals, which in turn at least partly compensated for the *pan* RNAi induced reduction in growth detected in the preceding prepupal growth phase.

pan RNAi Effects on Head Horn Development in *O. sagittarius*

O. sagittarius males exhibited significantly longer pupal head horns following *pan* RNAi compared to head horn length in control-injected pupae ($P = 0.0106$; Supporting Information Fig. 5; Supporting Information Table 9). Here, a small but significant difference in pupal male head horn length was also observed between control-injected and wild-type animals ($P = 0.0078$); however, both control groups differed significantly from *pan* RNAi individuals ($P = 0.0005$). In contrast, pupal head horn length in females showed no significant effect (Supporting Information Fig. 5; Supporting Information Table 9). Furthermore, adult head horn length in both sexes showed no significant change after *pan* RNAi (Supporting Information Fig. 5; Supporting Information Table 9). Interestingly, absolute and relative pupal head horn loss were significantly elevated in *pan* RNAi males ($P = 0.0089$ and $P = 0.0184$, respectively; Supporting Information Table 10), suggesting that the elevated growth of head horns observed in these males was compensated for by enhanced resorption, resulting in adult horns indistinguishable from control individuals.

DISCUSSION

Here, we show that a transcription factor in the Wnt pathway is involved in the sex- and location-specific development of a novel structure, the beetle horn. Specifically, we observed that in *O. binodis*, *pan* RNAi affected both prepupal pronotal horn growth and pupal horn remodeling in both sexes, which together resulted in significantly reduced pronotal horns in adults. In contrast, in *O. sagittarius* we detected no significant effect of *pan* RNAi on prepupal pronotal horn growth and were able to detect a significant reduction of pupal remodeling only in female *O. sagittarius*. Despite rather modest effects of *pan* RNAi on specific phases of pronotal horn development in this species, the resulting adults expressed significantly reduced pronotal horns in both sexes, similar to *O. binodis*. In addition, we found that *pan* RNAi increased head horn growth in male but had no effect on the much larger-horned female *O. sagittarius*. Lastly, our results indicate that *pan* plays an important role in the development of wings, eyes, and limbs. Combined, our findings suggest that beetle horn development is regulated by members of the Wnt pathway and that species and sexes may diverge in the extent and developmental timing of this regulation. Below we briefly discuss the most important implications of our results.

pan Regulates Growth and Remodeling of Pronotal Horns Differently among Species and Sexes

We observed a significant reduction in pupal pronotal horn length only in *O. binodis* but not in *O. sagittarius* (Fig. 5). Recall that quantitative RT-PCR results showed substantially higher levels of *pan* transcript depletion in *O. sagittarius* compared to *O. binodis*. These observations suggest that the absence of a *pan* RNAi-induced effect on prepupal horn growth in *O. sagittarius* may not be explained simply by a failure to sufficiently deplete *pan* transcript abundance. Instead, these observations raise the possibility that *pan* may regulate growth of prepupal pronotal horns differently in the two species. However, we cannot exclude the possibility that *pan* does in fact regulate prepupal pronotal horn growth in *O. sagittarius* yet requires much stronger levels of transcript depletion relative to *O. binodis* to reveal this regulation in RNAi experiments.

Analyses of pupal horn loss similarly indicated a more pronounced effect of *pan* RNAi during pupal horn remodeling in *O. binodis* compared to *O. sagittarius* (Supporting Information Tables 7 and 8). Importantly, regardless of the species-specific differences in the effects on prepupal and pupal aspects of pronotal horn formation, the resulting adults of both species and sexes showed significantly reduced pronotal horns following *pan* RNAi (Fig. 5). Combined, these results suggest that *pan* affects pronotal horn development in both species but may do so by affecting initial growth and subsequent resorption differently depending on species or sex (summarized in Fig. 6).

pan Regulates Growth and Remodeling of Head Horns in Male but not Female *O. sagittarius*

The growth and remodeling of the large medial, more posterior head horn of female *O. sagittarius* was

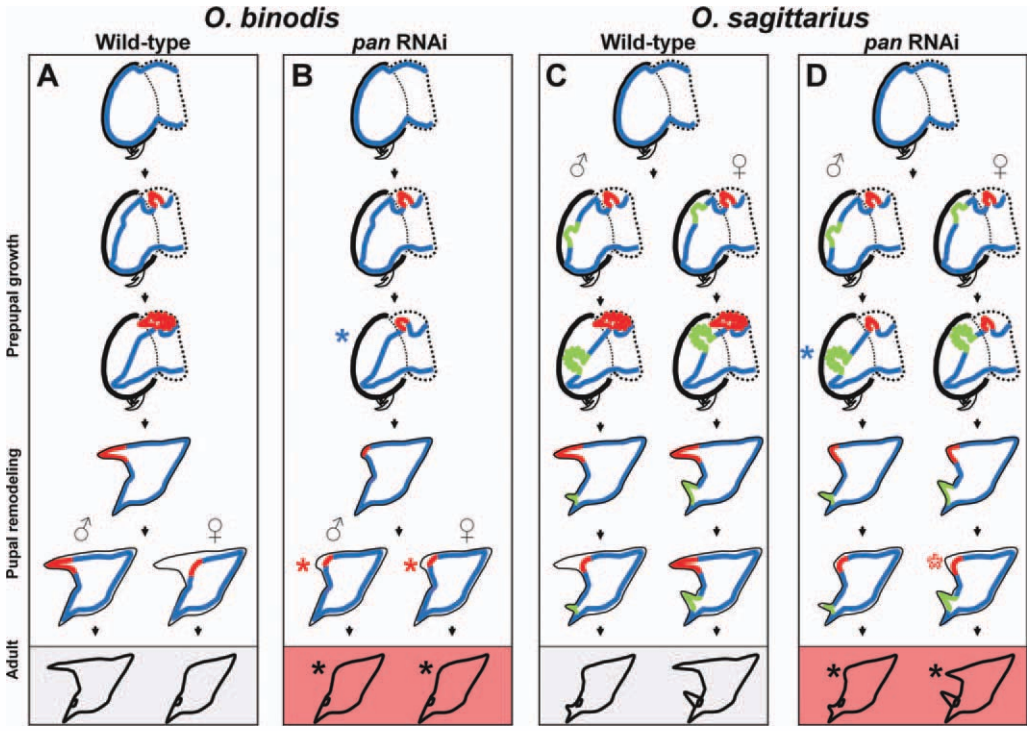

FIG. 6. Summary of *Onthophagus* horn growth and remodeling following *pan* RNAi. Illustrated (top to bottom) are pronotal and head horn development from larva to adult. Black lines denote larval and pupal cuticle, blue lines denote epidermal tissue, red lines denote pronotal horn tissue, and green lines denote head horn tissue (*O. sagittarius* only). Colored asterisks (*) indicate statistically significant changes between *pan* RNAi and control individuals in pupal horn length (blue), pupal horn remodeling (red), or adult horn length (black). (**a**) Wild-type *O. binodis* pronotal horn development with differential pupal horn resorption in males and females. (**b**) *O. binodis* pronotal horn development after *pan* RNAi with both decreased prepupal horn growth and decreased pupal horn resorption in both sexes. (**c**) Wild-type *O. sagittarius* pronotal and head horn development with pupal pronotal horn resorption among males and females. (**d**) *O. sagittarius* pronotal and head horn development after *pan* RNAi, with no statistically significant reduction in prepupal pronotal horn growth in both sexes, but increased head horn growth in males only. Also indicated are increased pupal head horn resorption in males and a significant decrease in relative pronotal horn resorption in females (asterisk with red outline). Finally, both sexes exhibit reduced adult pronotal horn length following *pan* RNAi.

entirely unaffected by *pan* RNAi. In contrast, male *O. sagittarius* expressed significantly longer pupal head horns following *pan* RNAi (Supporting Information Fig. 5). Recall that in male *O. sagittarius* head horn expression is limited to a pair of small, anterior horns. Our results thus raise the possibility that *pan* may regulate head horn growth in a location-specific manner and may have a stronger influence on anterior head horns compared to medial-posterior horns. More generally, our results suggest that head and pronotal horn development are at least partially decoupled.

Interestingly, the elevated head horn growth observed in male *pan* RNAi *O. sagittarius* was followed by a period of elevated horn resorption during the pupal stage. The latter effect fully compensated for the former, resulting in male adults with no discernible alteration of head horn length. This suggests that *pan* may directly regulate aspects of both the horn growth and resorption developmental processes. Alternatively, separate processes occurring during the pupal remodeling phase are able to recognize and compensate for incorrect horn growth that occurred during the prepupal stage. A compensatory interaction between effects on prepupal growth and pupal remodeling were also observed for pronotal horns in *O. binodis*, albeit in the opposite direction: both prepupal growth and pupal resorption were reduced, partly compensating for each other. Similar observations have also been made in previous studies (Moczek and Rose, 2009; Wasik and Moczek, 2011).

pan Regulates Growth of Non-horn Appendages and Sensory Structures

Apart from its effects on horn development, *pan* RNAi resulted in many shared and unique additional phenotypes in both species. *pan* RNAi phenotypes shared by both species included reduced elytra and reduced or abnormal tarsi (see Fig. 4). In contrast, eye width was affected only in *O. binodis,* and fore-tibia length was significantly reduced only in *O. binodis* males (Supporting Information Figs. 3 and 4).

pan RNAi phenotypes observed in this study were similar to adult *pan* phenotypes seen in studies on *Drosophila*, such as reduced or abnormal leg and wing appendages. Moreover, our results are consistent with a subtle role of *pan* in adult eye development in at least one species, *O. binodis*, again matching results from previous work on *Drosophila* (Brunner *et al*., 1997). In contrast, even though *pan* was expressed widely throughout the larval thoracic epithelium, we did not observe any limb bifurcations, reduced antennae or any obvious elytra-to-notum transformations, otherwise common phenotypes in adult *wg* and *pan Drosophila* null mutants (Fig. 2; Brunner *et al.*, 1997; Morata and Lawrence, 1977). This may be indicative of evolved differences in *pan* function between *Drosophila* and *Onthophagus*, or perhaps more likely, incomplete elimination of *pan* transcripts following larval RNAi in our study.

METHODS

Rearing Conditions

O. binodis and *O. sagittarius* were reared in colonies at Indiana University, and colony maintenance, breeding, and sexing were done as previously described (Moczek and Nagy, 2005; Wasik and Moczek, 2011).

pan Cloning and Sequence Analysis

O. binodis pan (*Obpan*) was isolated through PCR using an *O. binodis* cDNA library as a template. Degenerate, nested forward primers were designed to nucleotides encoding amino acids 477–484 and 485–492 in *Tribolium castaneum pan* (*Tcpan*; GenBank Accession: NM_001039401). Degenerate, nested reverse primers were designed to nucleotides encoding 576–582 and 585–591 in *Tcpan*. Primers were designed using primer sequences that amplified the 5′ and 3′ regions of an *Oncopeltus fasciatus* pan protein (*Of*pan; generously provided by Dr. David Angelini; GenBank Accession: AAW82622). *O. sagittarius pan* (*Ospan*) was obtained from nested PCR reactions with cDNA with degenerate forward primers designed to nucleotides encoding amino acids 477–484 and 485–492 and reverse primers designed to nucleotides encoding amino acids 557–564 and 538–544 in *Tc*pan. Both *Obpan* and *Ospan* PCR products were cloned into a pSC-A vector with a Strataclone PCR Cloning kit (Stratagene) and sequenced (Moczek and Rose, 2009). Since completion of this study, a more upstream region of *pan* has been identified independently through high-throughput sequencing in another *Onthophagus* species, *O. taurus* (see Choi *et al.*, 2010).

Upon sequencing of the *pan* region described in this study, two *pan* isoforms were discovered in both *Onthophagus* species matching sequences documented in *Drosophila* (see Dooijes *et al*., 1998) but not *Tribolium* or *Oncopeltus*. As a result, only *pan* regions shared across isoforms were used for in situ hybridization, dsRNA construction, and quantitative RT-PCR primer construction (described below). *pan* isoforms from both species were submitted to GenBank (*ObpanA*: HM632026, *ObpanB*: HM632028, *OspanA*: HM632027, *OspanB*: HM632029). Nucleotide and amino acid alignments were generated with Clustal X (Thompson *et al.*, 1997).

In situ Hybridization

DIG-labeled (Roche, IN) sense and antisense RNA probes were constructed from the first 180 bp in all *Obpan* and *Ospan* sequences and then synthesized with RNA polymerases from MEGAscript High Yield Transcription Kits (Applied Biosystems/Ambion, TX). RNA probes were used on sagittal, prepupal larval cryosections of both *Onthophagus* species, and in situ hybridization reactions were performed as in previous studies (Wasik and Moczek, 2011; Wasik *et al.*, 2010).

dsRNA Construction and Injection

dsRNA constructs for *Obpan* and *Ospan* were created from the same nucleotide region as the RNA probe (black box in Supporting Information Figs. 1B,C and 2B,C). In vitro transcription and injection of *Obpan*, *Ospan*, and control dsRNA constructs generated from BlueScript plasmid vector sequence (167 bp portion) were done with T7 and T3 RNA polymerases per manufacturer instructions (MEGAscript kit, Ambion), similar to previous studies (Moczek and Rose, 2009; Wasik *et al.*, 2010). Both antisense and sense RNA were combined in equal concentrations, heated to 95°C for 3 min, cooled gradually over 4 h until reaching −25°C, and then stored at −20°C until injection. *Onthophagus* larvae were injected with dsRNA (Bluescript plasmid or ds*pan*) at the beginning of the 3rd instar, following the protocol described in previous studies (Moczek and Rose, 2009; Wasik and Moczek, 2011; Wasik *et al.*, 2010). Post injection, adults in all treatment groups were weighed on the 2nd day of adulthood, preserved in 70% EtOH, and stored at −20°C.

Tissue Collection

Tissue samples from the dorsal prothorax from both species and sexes were collected within 24 h of pupation from wild-type animals, in addition to *pan* RNAi animals with effects on both morphology and allometric measurements. Thoracic tissue was dissected and stored as described in Wasik and Moczek (2011).

RNA Extraction and cDNA Synthesis

RNA extractions from dissected pupal prothoracic tissue were done with the RNeasy Mini Kit and RNase-

Free DNase Set (Qiagen; Alameda, CA) with the modifications described in Wasik and Moczek (2011). RNA and cDNA concentrations, along with cDNA synthesis, were also done as described in Wasik and Moczek (2011). *O. binodis* cDNA samples were collected from five wild-type females and males, and five *pan* RNAi females and males. *O. sagittarius* cDNA thoracic tissue samples were collected from four wild-type females and males, and four *pan* RNAi females and males.

Quantitative RT-PCR Analyses

pan quantitative RT-PCR primers were designed with Oligoanalyzer and PrimerQuest/Primer3 (Table 6; Integrated DNA Technologies; Rozen and Skaletsky, 2000). Primer optimization for effective reaction concentration along with standard curve measurements and negative controls in both primer tests and quantitative RT-PCR reactions were done as described in Wasik and Moczek (2011). Similarly, quantitative RT-PCR reactions were performed with a Stratagene MX3000P system (Stratagene/Agilent; Santa Clara, CA) at Indiana University using SYBR Green and ROX dyes for fluorescence readings and ROX as the reference dye. The thermal profile used was identical to that described in Wasik and Moczek (2011) with one exception in Segment 2, which consisted of 50 cycles with a 15 s decline to 94°C, 30 s at 53°C for *O. binodis* samples or 52°C in *O. sagittarius* samples, followed by 30 s at 72°C with endpoint data collection. Quantitative RT-PCR of all tissue was replicated, and results were analyzed as detailed in Wasik and Moczek (2011).

Two-tailed *t*-tests were used to determine significant differences in *pan* expression levels and were normalized to *O. binodis* and *O. sagittarius β-actin* (Wasik and Moczek, 2011) using the formula ($C_{t\ pan}/C_{t\ actin}$) among wild type and *pan* RNAi individuals in each species (see Barmina and Kopp, 2007). Relative expression fold differences were calculated with the $2\text{^}{-\Delta\Delta Ct}$ equation (Livak and Schmittgen, 2001; Schmittgen and Livak, 2008) with C_t values from tissue samples of both wild type and *pan* RNAi individuals inputted such that $\Delta\Delta C_t = (C_{t\ pan} - C_{t\ actin})_{wild\text{-}type} - (C_{t\ pan} - C_{t\ actin})_{pan\ RNAi}$. C_t values were then averaged for each of the treatment groups ($n = 5$ for *O. binodis* and $n = 4$ for *O. sagittarius*).

Allometric Measurements

Pupal and adult fore-tibia, pronotal horn, and head horn length were measured as previously described (Moczek and Rose, 2009; Wasik *et al.*, 2010). Eye width was measured as the average width of right and left dorsal eyes. All measurements were recorded to the nearest 0.001 mm and graphed with SigmaPlot (v. 7.0, SPSS Inc., Chicago, IL).

Pupal measurements in all treatment groups were used to evaluate whether *pan* RNAi affected horn growth during the prepupal phase. However, adult horn expression is also affected by pupal resorption, which follows prepupal growth and which may be independently influenced by *pan* RNAi. Two additional analyses were therefore conducted, detailed in Moczek (2006) and Wasik and Moczek (2011), which permit the quantification of changes in adult horn length specifically resulting from pupal resorption. Briefly, we calculated "absolute horn loss" and "relative horn loss" by comparing pupal and adult measurements of the same individual to quantify the degree to which pupal scaling relationships were either retained into the adult stage or modified due to differential horn resorption. By comparing pupal horn lengths on one side, and both measures of horn resorption on the other, we were, therefore, able to evaluate whether *pan* RNAi affected adult horn expression solely by affecting prepupal horn growth, pupal horn resorption, or both.

Statistical Analyses

ANOVAs were performed similar to those described in Wasik and Moczek (2011). Treatment (RNAi, control-injected, and wild type) and mass × treatment interactions were used as model effects. The significance of absolute and relative horn loss were also tested with ANOVAs (Moczek, 2006). For all statistical analyses, wild-type and control-injected animals did not differ significantly in any measurements, unless otherwise noted in the results. Only measurements from adults with obvious *pan* RNAi phenotypes were used for RNAi treatment analyses, as explained in the results below.

ACKNOWLEDGMENTS

The authors thank two anonymous reviewers, Dr. David Angelini for providing primer sequences, Dr. Justin Kumar for access to a NanoDrop 1000 Spectrophotometer, and the Center for Genomics and Bioinformatics at Indiana University for quantitative RT-PCR resources. Additionally, they thank Erin Yoder for expert beetle care and Will Haines for collecting and shipping *O. sagittarius* from the field.

LITERATURE CITED

Angelini DR, Kaufman TC. 2005a. Functional analyses in the milkweed bug *Oncopeltus fasciatus* (Hemiptera) support a role for Wnt signaling in body segmentation but not appendage development. Dev Biol 283:409–423.

Angelini DR, Kaufman TC. 2005b. Insect appendages and comparative ontogenetics. Dev Biol 286:57–77.

Arrow GJ. 1951. Horned beetles, a study of the fantastic in nature. The Hague: W. Junk.154 p.

Baker N. 1988. Transcription of the segment-polarity gene wingless in the imaginal discs of *Drosophila*, and the phenotype of a pupal-lethal *wg* mutation. Development 102:489–497.

Baratte S, Peeters C, Deutsch J. 2006. Testing homology with morphology, development and gene expression: Sex-specific thoracic appendages of the ant *Diacamma*. Evol Dev 8:433–445.

Barmina O, Kopp A. 2007. Sex-specific expression of a HOX gene associated with rapid morphological evolution. Dev Biol 311:277–286.

Bejsovec A. 2006. Flying at the head of the pack: Wnt biology in *Drosophila*. Oncogene 25:7442–7449.

Bolognesi R, Farzana L, Fischer TD, Brown SJ. 2008. Multiple Wnt genes are required for segmentation in the short-germ embryo of *Tribolium castaneum*. Curr Biol 18:1624–1629.

Brunner E, Peter O, Schweizer L, Basler K. 1997. *pangolin* encodes a Lef-1 homologue that acts downstream of Armadillo to transduce the Wingless signal in *Drosophila*. Nature 385:829–833.

Carroll SB, Gates J, Keys DN, Paddock SW, Panganiban GE, Selegue JE, Williams JA. 1994. Pattern formation and eyespot determination in butterfly wings. Science 265:109–114.

Chang M, Chang J, Gangopadhyay A, Shearer A, Cadigan K. 2008. Activation of wingless targets requires bipartite recognition of DNA by TCF. Curr Biol 18:1877–1881.

Choi JH, Kijimoto T, Snell-Rood E, Tae H, Yang Y, Moczek AP, Andrews J. 2010. Gene discovery in the horned beetle *Onthophagus taurus*. BMC Genomics 11:703.

Diaz-Benjumea F, Cohen B, Cohen S. 1994. Cell interaction between compartments establishes the proximal-distal axis of *Drosophila* legs. Nature 372:175–179.

Dooijes D, van Beest M, van de Wetering M, Boulanger G, Jones T, Clevers H, Mortin M. 1998. Genomic organization of the segment polarity gene *pan* in *Drosophila melanogaster*. Mol Gen Genet 258:45–52.

Emlen DJ, Marangelo J, Ball B, Cunningham CW. 2005. Diversity in the weapons of sexual selection: Horn evolution in the beetle genus Onthophagus (Coleoptera: Scarabaeidae). Evolution 59:1060–1084.

Grossmann D, Scholten J, Prpic N. 2009. Separable functions of *wingless* in distal and ventral patterning of the *Tribolium* leg. Dev Genes Evol 219:469–479.

Hulo N, Bairoch A, Bulliard V, Cerutti L, De Castro E, Langendijk-Genevaux P, Pagni M, Sigrist C. 2006. The PROSITE database. Nucleic Acids Res 34:D227–D230.

Livak K, Schmittgen T. 2001. Analysis of relative gene expression data using real-time quantitative PCR and the 2(-Delta Delta C(T)) Method. Methods 25:402–408.

Logan C, Nusse R. 2004. The Wnt signaling pathway in development and disease. Annu Rev Cell Dev Biol 20:781–810.

Moczek AP. 2006. Pupal remodeling and the development and evolution of sexual dimorphism in horned beetles. Am Nat 168:711–729.

Moczek AP, Nagy LM. 2005. Diverse developmental mechanisms contribute to different levels of diversity in horned beetles. Evol Dev 7:175–185.

Moczek AP, Rose DJ. 2009. Differential recruitment of limb patterning genes during development and diversification of beetle horns. Proc Natl Acad Sci USA 106:8992–8997.

Morata G, Lawrence P. 1977. The development of *wingless*, a homeotic mutation of *Drosophila*. Dev Biol 56:227–240.

Ober KA, Jockusch EL. 2006. The roles of *wingless* and *decapentaplegic* in axis and appendage development in the red flour beetle, *Tribolium castaneum*. Dev Biol 294:391–405.

Rozen S, Skaletsky HJ. 2000. Primer3 on the WWW for general users and for biologist programmers. In: Krawetz S, Misener S, editors. Bioinformatics methods and protocols. Totowa, NJ: Humana Press. pp365–386.

Schmittgen T, Livak K. 2008. Analyzing real-time PCR data by the comparative C(T) method. Nat Protoc 3:1101–1108.

Snell-Rood EC, Moczek AP. Horns, hormones, and hox genes: The role of development in the evolution of beetle contests. In: Hardy I, Briffa M, editors. Animal contests. UK: Cambridge University Press. in press.

Thompson JD, Gibson TJ, Plewniak F, Jeanmougin F, Higgins DG. 1997. The CLUSTAL_X windows interface: Flexible strategies for multiple sequence alignment aided by quality analysis tools. Nucleic Acids Res 25:4876–4882.

van de Wetering M, Cavallo R, Dooijes D, van Beest M, van Es J, Loureiro J, Ypma A, Hursh D, Jones T, Bejsovec A, Peifer M, Mortin M, Clevers H. 1997. Armadillo coactivates transcription driven by the product of the *Drosophila* segment polarity gene *dTCF*. Cell 88:789–799.

Wasik BR, Moczek AP. 2011. *decapentaplegic* (*dpp*) regulates the growth of a morphological novelty, beetle horns. Dev Genes Evol 221:17–27.

Wasik BR, Rose DJ, Moczek AP. 2010. Beetle horns are regulated by the *Hox* gene, *Sex combs reduced*, in a species- and sex-specific manner. Evol Dev 12:353–362.

Werner T, Koshikawa S, Williams T, Carroll S. 2010. Generation of a novel wing colour pattern by the Wingless morphogen. Nature 464:1143–1148.